Finite Element Analysis of Contact Stress Distribution on Insert Conformity Design of Total Knee Arthroplasty

Techin Seechaipat, Supakit Rooppakhun(✉), Chotchuang Phombut
Suranaree University of Technology, Nakhon Ratchasima, Thailand
`supakit@sut.ac.th`

Abstract—The tibial insert conformity is one of the essential parameters concerned with the contact stress distribution of biomechanics characteristics in total knee arthroplasty (TKA). This study aimed to evaluate the effect of tibial insert conformity design on contact stress distribution using Finite Element (FE) analysis. The three-dimensional (3D) FE model of the posterior stabilized type of TKA was analyzed according to the standard knee implant loading. The 3^k factorial experimental design was performed for the response surface of different insert curvatures consisting of the curve, partial flat, and flat insert conformity in sagittal and coronal planes. According to the result, the coronal and sagittal plane conformity displayed the effect of the change on the contact stress, including the contact area for the flexion angle of the knee joint. The maximum contact stress increased while the contact area value decreased during the flexion angle of the knee joints raised. The changing insert conformity value in the sagittal plane displayed higher sensitivity to contact stress than the changing conformity in the coronal plane. The relationship between the contact stress and tibial insert conformity under knee flexion angle indicates highly regression suitable for the prediction. In addition, the FE simulation result was then verified by compared to mechanical testing using the Fujifilm technique. The result of FE analysis exhibited similar to that of the mechanical test. The study indicated that the different geometric designs of the insert conformity played a crucial role that influenced and relationship to the contact stress of TKA.

Keywords—insert conformity, total knee arthroplasty, contact stress, finite element analysis

1 Introduction

Total knee arthroplasty (TKA) is an orthopedic surgical procedure widely used to treat osteoarthritis to relieve pain by repairing the weight-bearing surfaces of the knee joint. However, there are still reports of complications from patients after surgery due to problems, such as implant loosening, pain, and weight-bearing surface wear [1]-[3]. The surface wear of the insert component is an essential factor for the shortening lifetime included the loosening of TKA [4]-[7]. In extreme situations, revision surgery may be required because of material damage, which generally uses Ultra-High Molecular Weight Polyethylene (UHMWPE) material. Previous studies have found that the wear

rate of the tibia insert is related to the changing of the contact stress on the articular surface [4]-[6]. The contact mechanics on the tibial insert of TKA is caused by various factors, including material, geometry design, patient activity levels. The geometric conformity related to the radii ratio between the femoral component and the tibial insert is an essential factor influencing contact stress and area in TKA design [8]-[10]. The tibial insert conformity is a crucial parameter related to both the coronal and sagittal plane for TKA, which should be considered in both biomechanics contact and wear performance [4]-[7]. The high conformity design of TKA produces low contact stress provided does not exceed the fatigue limit of the material, including a wide contact area reducing surface wear. In addition, the contact stress distribution correlates inversely to the contact area of the insert component related to the load under the flexion angle of the knee joint. It was discovered to directly affect contact pressure under various loads, resulting in material wear [11].

The effect of conformity is significant in the determination of TKA wear, including biomechanical performance, according to the previous study with the computational model using Finite Element (FE) analysis and experiments [12]-[16]. Using FE analysis, the biomechanics contact between the articulating against of insert and a femoral component could be described as reliable as the experimental study. In addition, in vitro study of contact pressure distribution in the tibiofemoral using Fujifilm technique or Tekscan pressure sensor was a standard instrument, which helps to understand the impact of geometric design of TKA [17],[18]. However, the experimental studies still have a high cost and long-time limitation. According to the knee contact pressure test, the purpose of the standard was to evaluate the pressure distribution and total contact area on the tibiofemoral joint of the TKA system based on the bodyweight load in each different flexion angle [19]. The bearing load in each flexion angle of 0 to 90 degrees with the loading in the range of 4 to 5 times of body weight was used to determine the knee contact pressure. The results can be used to develop optimized geometries that include the insert conformity.

The design of experiments (DOE) was generally used to evaluate the main factor affecting the output, leading to the optimized output response and explanation of the interaction between the factors [20]. The purpose of responses surface methodology (RSM) was to determine the optimal condition system by analyzing multi-factor data that evaluated the level of factors that optimize the response. Previous studies have used an optimization method to determine the positioning parameters of TKA. The relationship of biomechanical parameters such as varus angle, posterior slope angle, and external rotation angle reduces the peak value of pressure [21]. This study hypothesizes that the various conformity ratio in TKA changes the insert curvature effect on the contact stress and area.

Therefore, this study aimed to investigate the effect of insert conformity design to the contact stress based on FE analysis. The full factorial DOE was performed with a different design of conformity consisting of a curved, partial flat, and flat in the sagittal and coronal planes. The surface response analysis was also evaluated between the contact stress distribution and the tibial insert conformity. In addition, the mechanical test

was performed to validate of FE simulation. The results of this study provide information concerned with the relation of contact stress and conformity design of the TKA tibial insert component.

2   Materials and methods

2.1   3D finite element model

This study created the 3D computational model of a posterior-stabilized TKA consisting of the femoral and tibial insert components, as shown in Figure 1(a). The tibial insert conformity was defined by the ratio of geometric curvature radius between the femoral and tibial insert components in the sagittal plane (Cs) and the coronal plane (Cc), as illustrated in Figure 1(b). Table 1 shows the three-level experimental design of the conformity parameter in the coronal and sagittal planes, consisting of the curve, partial curve, and flat.
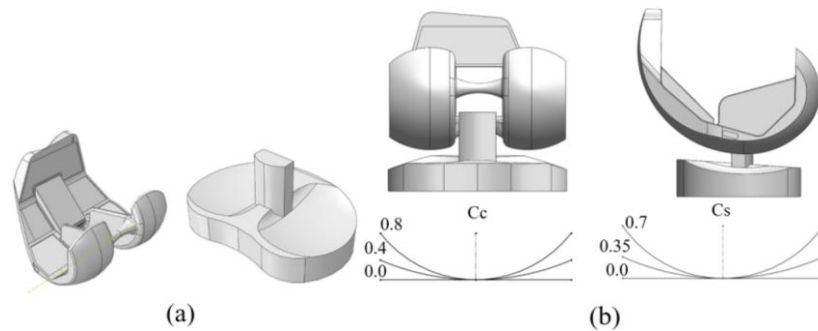

Fig. 1. (a) The 3D model of femoral (left) and tibial insert component (right); (b) The tibial insert conformity consisted of the coronal plane (Cc) and sagittal plane (Cs)

Table 1. The tibial insert conformity values according to the sagittal and coronal planes

Parameters		Abbreviation	Values
Coronal Conformity (Cc)	Curve	Cc_{max}	0.80
	partial flat	Cc_{mid}	0.40
	Flat	Cc_{min}	0.00
Sagittal Conformity (Cs)	curve	Cs_{max}	0.70
	partial flat	Cs_{mid}	0.35
	flat	Cs_{min}	0.00

The FE model of a rigid body femoral component and the deformed body of the tibial insert component was created and analyzed using the computer simulation software (Abaqus Knee Simulator-SIMULIA, Johnston, USA). The mechanical properties of the tibial insert component were considered by the elastic modulus of 685 MPa, Poisson ratio of 0.47, and the density of 0.94 g/cm^3 [22].

This study performed mesh convergence testing to verify that the FE result was significantly independent according to mesh refinement. The element size was considered between 3.5 mm to 0.5 mm until the different percentages changing of maximum contact stress was less than 2%, as shown in Figure 2. The convergence results indicated that the mesh density utilized for these insert components was an acceptable range relative to that obtained in a previous study [23], [24].
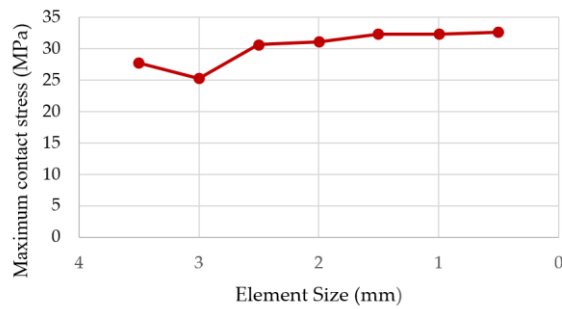

Fig. 2. The mesh convergence test for the FE result of maximum contact stress

2.2 Boundary and loading conditions

Figure 3 shows the boundary conditions of FE analysis. The vertical load was performed on the surface of the femoral component based on the equal distribution on the medial and lateral sides. The bottom surface of the tibial insert component was considered fully constrained with no translation and rotation. The femoral component was allowed free moving in the medial-lateral (ML) translation, including the internal-external (IE) and varus-valgus (VV) rotations. The friction coefficient between the femoral and tibial insert components was 0.04 [13].

Fig. 3. Boundary and loading conditions

The FE analysis was performed under various flexion angles between the femoral and tibial insert components. Table 2 displays the applied load according to the flexion angle of the knee joint according to the standard specifications for testing a knee replacement prosthesis (ASTM F2083) [19].

Table 2. The load and flexion angles according to the standard testing [19]

Flexion angle (degrees)	Load (kN)
0	2,901
15	2,901
30	3,267
60	3,626
90	3,267

2.3 Response surface methodology

The design of experiment (DOE) affected the statistical design and analysis process, including the screening design and optimization [20]. The optimization design method is generally analyzed for finding a response optimizer to determine the optimum factor value. In this study, response surface methodology (RSM) was performed based on a three-level (3^k) full factorial design. The data were examined to determine the optimal tibial insert conformity based on the average pressure distribution and gait cycle pressure level. The previous studies revealed that the magnitude of contact stress distribution on the tibiofibular joint was in a range of 15 to 30 MPa [21],[23],[25].

2.4 Experiment for the validation of FE results

For the FE validation, the customized design of TKA consisting of femoral and tibial insert components obtained from our previous study was used [10]. The universal testing machine (UTM) (INSTRON-5565) and a specifically designed jig consisting of the upper and lower fixtures were used, as shown in Figure 4. The upper fixture could be the freedom of movement in translational and rotation varus and valgus. The applied load was controlled with equal distribution evenly in the medial and lateral parts of the tibial insert. The mono-sheet type of Fuji film (Medium pressure, Fuji Photo Film, Tokyo, Japan) was used with an operating capacity range of 10 MPa to 50 MPa, and a temperature range of 20° to 35°C. The compression load was performed withheld for 2 minutes and repeated three times.

The obtained Fuji film sheet was then used to scan under the high resolution of 1,000 dpi using color image scanner Epson A4 Perfection V37 (Epson, Perfection V37). The pressure distribution data were analyzed using the mapping system software (FPD-8010E, Fuji Photo Film, Japan) to quantify the contact stress and positioned on the contour outline of the tibial insert surface.
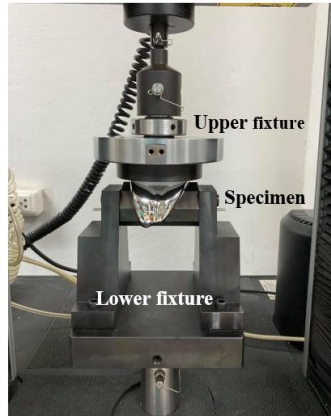
Fig. 4. The universal testing machine for experiment of contact stress distribution using Fuji film technique

3 Results

3.1 The contact stress distribution of various conformity

Figure 5 and Figure 6 illustrated the contact stress and the contact area in various flexion angles (0, 15, 30, 60, and 90 degrees) according to the changing conformity value of sagittal and coronal planes, respectively. The magnitude of contact stress increases when conformity decreases both in the sagittal and coronal planes decreases, including the increase of knee flexion angle. In contrast, the decrease in the contact area occurred in the case of low conformity at an increase in degree. The high conformity in the sagittal plane exhibited a low contact stress value, as shown in Figure 5(a). According to the contact area, the result was found that the flat conformity displayed high contact area. In contrast, the flat conformity revealed the high contact stress, as shown in Figure 5(b). In addition, the results showed that the tendency of changing contact stress and contact area following the conformity of the coronal plane displayed in Figure 6 similar changes in the conformity of the sagittal plane.
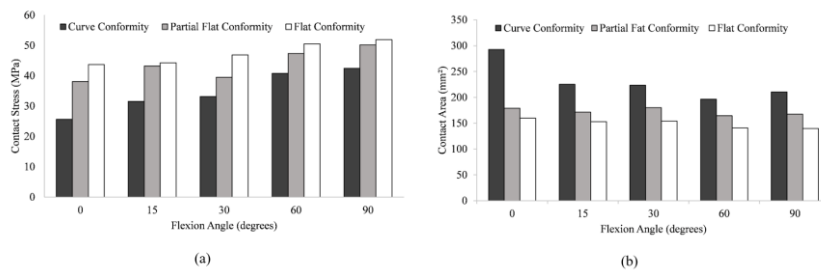

Fig. 5. The results of (a) contact stress and (b) contact area with changing sagittal conformity
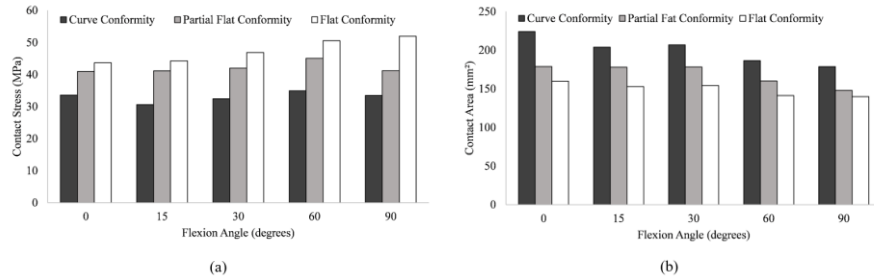
Fig. 6. The results of (a) contact stress and (b) contact area with changing coronal conformity

Figure 7 shows the result of contact stress distribution on the surface of the insert component according to the change of conformity at a flexion angle of 0 degrees. The contact stress distribution changed following the value of conformity which occurred a high value in a case of flat shape. Low conformity leads to high contact stress; however, it decreases with curved conformity. In a case of high conformity in the sagittal plane, the contact stress distribution exhibited the elongated elliptical shape in the anterior-posterior direction. Similarly, the contact stress was distributed laterally as an elliptical shape regarding the increase of coronal conformity.
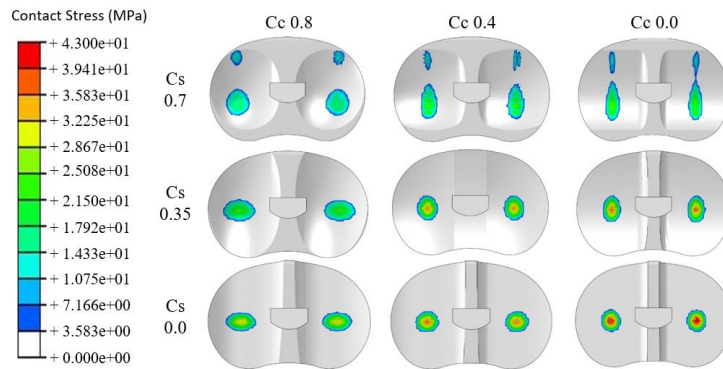

Fig. 7. The FE result of contact stress distribution on the tibial insert component with a change of conformity at a flexion angle of 0 degrees

3.2 Analysis of variance and response surface methodology

Table 3 shows the typical analysis of variance on the contact stress with the R-square value of 98.14 %. The Adj-R-square value of the contact stress indicating that the studied data was sufficient for analysis of the experiment was also similar to R-square. The variance analysis of insert conformity revealed that the Cc and Cs had a significant statistical ($p < 0.05$) effect on the contact stress. In addition, the interaction between the parameter of Cc and Cs was not statistically significant ($p > 0.05$) to the contact stress.

Table 3. Variance analysis of contact stress

Source	DF	Adj SS	Adj MS	F-Value	P-Value
Model	5	525.35	105.07	31.64	0.008
Linear	2	505.65	252.82	76.14	0.003
Cc	1	143.16	143.16	43.12	0.007
Cs	1	362.48	362.48	109.17	0.002
Square	2	17.18	8.59	2.59	0.222
Cc*Cc	1	16.20	16.20	4.88	0.114
Cs*Cs	1	0.97	0.97	0.29	0.626
2-Way Interaction	1	2.52	2.52	0.76	0.447
Cc*Cs	1	2.52	2.52	0.76	0.447
Error	3	9.96	3.32		
Total	8	535.31			

S = 1.82221 R-sq = 98.14% R-sq(adj) = 95.04% R-sq(pred) = 79.63%

Tables 4 show the regression analysis between the contact stress and insert conformity in various flexion angles. The R-square value of the relationship equation between Cc and Cs correlated to the contact stress was in the range of 97.34% to 98.16%. Figure 8 demonstrates the main effect of contact stress between coronal and sagittal planes conformity. The results showed that the Cs were more significantly related to contact stress than Cc. It can be drawn that the conformity change in the sagittal plane was more sensitive to changes in contact stress than the coronal plane.

Table 4. Regression analysis of contact stress and insert conformity

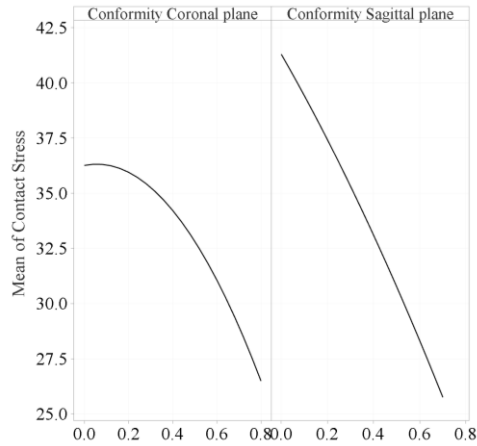| Flexion angle (degrees)	Equation	R-square (%)
0	44.12 + 0.03 Cc - 20.50 Cs - 17.79 Cc*Cc - 5.7 Cs *Cs + 5.68 Cc *Cs	98.14
15	45.41 - 6.04 Cc - 6.46 Cs - 17.51 Cc*Cc - 17.1 Cs*Cs + 12.56 Cc*Cs	97.34
30	46.34 + 0.95 Cc- 23.66 Cs - 23.57 Cc*Cc + 8.73 Cs*Cs + 6.43 Cc*Cs	97.98
60	50.39 - 2.04 Cc - 10.13 Cs - 20.27 Cc*Cc - 3.05Cs*Cs + 4.55 Cc*Cs	98.16
90	46.74 - 8.2 Cc - 2.1 Cs - 25.9 Cc*Cc + 36.8 Cs*Cs + 9.7 Cc*Cs	98.08

Fig. 8. The main effect plot for contact stress between coronal and sagittal conformity

Figures 9(a) and 9(b) displayed the response surface contour plots of Cs and Cc to contact stress and contact area, respectively. The results indicated that the contact stress could be reduced by increasing Cs and Cc. At the same time, the decrease of Cs and Cc has decreased contact area. From previous studies, the average maximum contact stress was approximately 30 MPa [25]. This consistency to Cs and Cc values was between 0.5 to 0.7 and 0.4 to 0.8, respectively. Also, the contact area to be valued was in the range of 220 mm^2 to 340 mm^2, as shown in Figure 9(b).
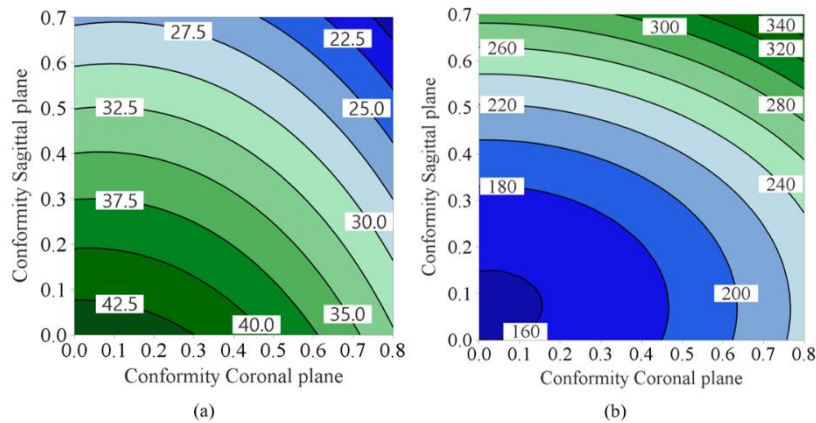

Fig. 9. The response surface of the tibial insert conformity to (a) Contact stress (unit: MPa) and (b) Contact area (unit: mm^2).

3.3 Validation of FE results

Figure 10 displays the mechanical testing result of contact stress distribution on the tibial insert surface obtained from the Fujifilm technique. Figures 11(a) and 11(b) exhibited the comparative result of average contact stress and contact area in 0 flexion angle between the FE analysis and Fuji film experiments. The FE result of the average contact stress displayed differences from the Fujifilm test, with 25.68 % and 29.21 % for the medial and lateral sides, respectively. The contact area difference between the FE analysis and the Fuji film test was shown for 1.94 % and 8.30 % for the center and lateral sides.
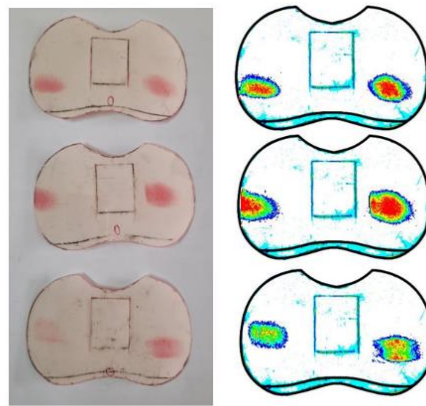

Fig. 10. The result of contact stress distribution obtained from the Fujifilm technique
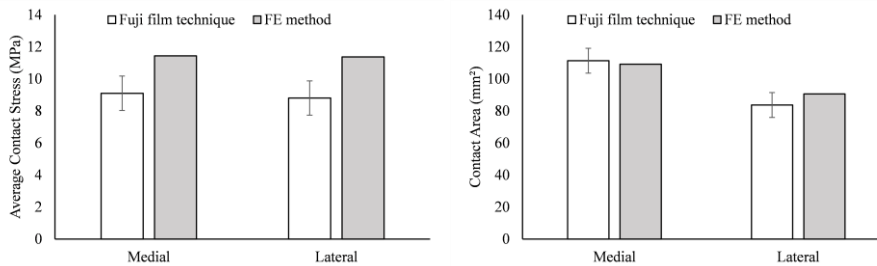

Fig. 11. The compared result between the Fuji film technique and FE analysis (a) average contact stress and (b) contact area

4 Discussion

Total knee arthroplasty (TKA) is a standard orthopedic surgical surgery that restores the articular surfaces of the knee joint to treat osteoarthritis. However, problems with implant loosening, pain, and weight-bearing surface wear are the most typical long-term complications of TKA. Most research reports that change in contact stress on the

articular surface is related to the wear rate of the tibia insert component, which is a critical factor for the limitation of longevity in TKA [4]-[6]. The contact stress on the TKA tibia insert is caused by various factors such as material, geometry design, the load level of patient activity [26]. The geometry conformity of the tibial insert is a crucial parameter related to both the coronal and sagittal plane for TKA, which should be considered in both biomechanics contact [4]-[7]. Generally, the conformity was defined as the radii ratio between the femoral component and the tibial insert in the coronal and sagittal planes [8]-[10]. A previous study of conformity variations was designed to determine the contact stress on tibial insert under various load conditions through experiments [25],[27].

This study evaluated the effect of differences in tibial insert conformity design to contact stress distribution and the contact area in the flexion angle and load based on the ASTM F2083 standard test. Three different insert conformities were investigated the main effect in the coronal and sagittal plane consisting of the curve, partial flat, and flat, including the response surface analysis. The increase of flexion angle carries out the contact stress increases, whereas the contact area decreases. Conformity change results show that the decrease of conformity value provides a high magnitude of contact stress with a low contact area [4]. Consequently, conformity design considerations were critical factors affecting the contact mechanisms on the tibial insert component. The previous studies suggested that the TKA be designed to reduce wear with low contact stress [8]-[9],[11]. The low magnitude of contact stress will increase the contact area. The high conformity design of the tibial insert affects the low contact stresses with an increased contact area [8]-[9],[11],[28].

The design of experiment (DOE) technique was generally used to create the starting point of the suitable sample in the simulation. The most common purpose of a screening design is to investigate the most critical factors affecting process quality, such as two-level full factorial designs and fractionate factorial designs. Following screening trials, optimization experiments are traditionally performed to provide more information on the relationship between the most relevant factors and the response variables [20]. This study used a three-level full factorial design method consisting of the design points of the tibial insert conformity were defined as high, medium, and low values in the coronal and sagittal plane were carried by using variance and RSM in the analysis. The variance analysis of the significance level to the contact stress at flexion angle 0 degrees, as exhibited in Table 3. This study found that analysis of variance of insert conformity found that the factor between Cc and Cs had a significant statistical ($p < 0.05$) effect on the contact stress. Furthermore, the interaction between factor Cc and Cs was not statistically significant ($p > 0.05$) to the contact stress. Table 4 shows the regression equations and R-square of contact stress at all flexion angles. All flexion angles represent a high R-square, indicating a highly suitable variable for predicting regression equations. Overall, a flexion angle of 0 degrees showed the most accurate prediction. The result also revealed that Cc and Cs interacted with the magnitude of the contact stress distribution. The Cs displayed a higher sensitivity to contact stress on the tibial insert component than Cc, as shown in Figure 8. It was consistent with the previous study, in which knee joint kinetics were significantly affected by the insert conformity design in the sagittal plane compared to the coronal plane. The conformity design of the inserts

in both the coronal and sagittal planes was important for determining the TKA knee kinematics [7].

The response surface method (RSM) was one of the most often used experimental designs for optimization, according to the optimum conformance design, because this allowed testing the effects of several factors on one or more responses [20],[29]. The magnitude of the contact stress distribution on the tibial insert ranged from 15 to 30 MPa [21],[23],[30]. The result corresponds to the contact stress in the previous report that displayed Cs and Cc ranging between 0.5 to 0.7 and 0.4 to 0.8, respectively. Also, the contact area was in the range of 220 mm^2 to 340 mm^2. The conformity in this study was consistent in the range of the previous study that designed an optimal conformity design of the tibial insert to reduce wear volume in TKA [31]. The result of high conformity was reduced contact stress, which decreases the pressure exerted on the tibial insert component [8],[11],[32]. Although the high conformity was provided the reduction of contact stress, fatigue, and wear on insert component, there may be some limitations such as constraint or mobility of TKA [6]. Biomechanical analyzes have suggested that high conformity may cause over-constraint of the knee joint during normal daily activities [6],[32]. For the design of TKA, it is necessary to consider other factors to complete the design of the TKA, such as material, constraint, the volume of wear.

In this study, the validation result of the average contact stress and contact area using FE analysis was compared with the Fuji film technique of the artificial tibiofemoral joint. Comparatively, the difference percentage of the contact area and average contact stress from measurements of Fuji film and simulated FE analysis displayed as 1.94% and 29.21%, respectively. Previous studies revealed the accuracy of Fuji film techniques assessed the contact stress distribution of the TKA displayed in a range of 6 % to 36% [30],[33]. Although the Fujifilm technique was variable, the significant advantage has been reviewed numerous times and is satisfied with various applications [34]. The FE analysis using computer simulation is a beneficial and widely accepted tool, especially varied conditions and investigated outcomes in biomedical applications. The low cost and periods were advantages of modeling and simulation techniques and predicting specific results that the experimental cannot be described.

This study has some limitations. The first was a femoral component model considered based on only one commercial model. The resulting contact stress may differ from other knee implant designs. Secondly, the study was evaluated the contact pressure distribution based on the assumption of static load. The actual load should be considered in dynamic loading such as the following standard loading profiles ASTM F3141. Future studies should be considered to provide the contact mechanisms of knee implants similar to the kinetic behavior of the normal knee joint. Finally, the load and displacement conditions of the knee joint should be considered by a system of muscles and ligaments that affect knee movement behavior included in the musculoskeletal system simulation model for further study.

5   Conclusions

This study evaluated the influence of insert geometric conformity design in both coronal and sagittal planes on the biomechanical contact of TKA. Using a three-level factorial design of the experiment, the factor of three different curvatures included curved, partial flat, and flat insert shapes, were analyzed. The results showed that the variation of insert conformity design affected the contact stress and the contact area during the flexion angle of the knee joint. The changing conformity in the sagittal planes displayed a more significant change in contact stress sensitivity than the conformity in the coronal plane. The results of the surface response analysis revealed that the high conformity resulted in low contact stresses while the contact area was increased. Regarding the validation, the FE analysis of contact stress and contact area was similar to the mechanical test using the Fuji film technique. The geometrical design of the insert component conformity significantly influenced and related to the contact stress of TKA.

6   Acknowledgment

7   References

[1] Ardestani, M., Moazen, M., maniei, E., and Jin, Z. (2015). Posterior stabilized versus Cruciate retaining Total Knee Arthroplasty designs: conformity affects the performance reliability of the design over the patient population. Medical Engineering & Physic, 37: 350-360. https://doi.org/10.1016/j.medengphy.2015.01.008

[2] Koh, Y.G., Nam, J.H., and Kang, K.T. (2018). Effect of geometric variations on tibiofemoral surface and post-cam design of normal knee kinematics restoration. Journal of Experimental Orthopaedics, 5: 53-65. https://doi.org/10.1186/s40634-018-0167-z

[3] Koh, Y. G., Son, J., Kwon, O. R., Kwon, S. K., and Kang, K. T. (2019). Tibiofemoral conformity variation offers changed kinematics and wear performance of customized posterior-stabilized total knee arthroplasty. Knee Surg Sports Traumatol Arthrosc, 27: 1213-1223. https://doi.org/10.1007/s00167-018-5045-9

[4] Abdelgaied, A., Brockett, C. L., Liu, F., Jennings, L. M., Jin, Z., and Fisher, J. (2014). The effect of insert conformity and material on total knee replacement wear. Proc Inst Mech Eng H, 228: 98-106. https://doi.org/10.1177/0954411913513251

[5] Galvin, A. L., Kang, L., Udofia, I., Jennings, L. M., McEwen, H. M., Jin, Z., and Fisher, J. (2009). Effect of conformity and contact stress on wear in fixed-bearing total knee prostheses. J Biomech, 42: 1898-1902. https://doi.org/10.1016/j.jbiomech.2009.05.010

[6] Brockett, C., Carbone, S., Fisher, J., and Jennings, L. (2017). Influence of conformity on the wear of total knee replacement: An experimental study. Proceedings of the Institution of

Mechanical Engineers, Part H: Journal of Engineering in Medicine, 232: 127-134. https://doi.org/10.1177/0954411917746433

[7] Zhang, Q., Chen, Z., Zhang, J., Hu, J., Peng, Y., Fan, X., and Jin, Z. (2019). Insert conformity variation affects kinematics and wear performance of total knee replacements. Clinical Biomechanics, 65: 19–25. https://doi.org/10.1016/j.clinbiomech.2019.03.016

[8] Banaszkiewicz, P. (2014). The Effect of Conformity, Thickness, and Material on Stresses in Ultra-High Molecular Weight Components for Total Joint Replacement. Classic Papers in Orthopaedics, 93-96. https://doi.org/10.1007/978-1-4471-5451-8_22

[9] Villa, T., Migliavacca, F., Gastaldi, D., Colombo, M., and Pietrabissa, R. (2004). Contact stresses and fatigue life in a knee prosthesis: comparison between in vitro measurements and computational simulations. J Biomech: 37: 45-53. https://doi.org/10.1016/s0021-9290(03)00255-0

[10] Phombut, C., Rooppakhun, S., and Sindhupakorn, B. (2021). Morphometric Analysis and Three-Dimensional Computed Tomography Reconstruction of Thai Distal Femur. Applied Sciences, 11: 1052. https://www.mdpi.com/2076-3417/11/3/1052

[11] Sharma, A., Komistek, R. D., Ranawat, C. S., Dennis, D. A., and Mahfouz, M. R. (2007). In vivo contact pressures in total knee arthroplasty. J Arthroplasty, 22: 404-416. https://doi.org/10.1016/j.arth.2006.07.008

[12] Usman, and Huang, S. C. (2017). Effect of Average Conformity on Contact Stresses in Total Knee Replacement: Finite Element Analysis. MATEC Web Conf., 108: 13006. https://doi.org/10.1051/matecconf/201710813006

[13] Shu, L., Sato, T., Hua, X., and Sugita, N. (2021). Comparison of Kinematics and Contact Mechanics in Normal Knee and Total Knee Replacements: A Computational Investigation. Ann Biomed Eng, 49: 2491-2502. https://doi.org/10.1007/s10439-021-02812-0

[14] Li, G., Liu, J., Jiang, G., Kong, J., Xie, L., and Li, Z. (2013). Simulation of Expansion Joint of Bottom Lining in Ladle and Its Influence on Thermal Stress. International Journal of Online and Biomedical Engineering (iJOE), 9: 5-8. https://doi.org/10.3991/ijoe.v9i2.2557

[15] Zainol, Z. N., Tap, M. M., Kamar, H. M., and Kamsah, N. (2019). Heat Transfer Model to Predict Human Skin Temperature under Comfort Level by using Bioheat Equation. International Journal of Online and Biomedical Engineering (iJOE), 15: 52-64. https://doi.org/10.3991/ijoe.v15i10.10876

[16] Kuriyama, S., Ishikawa, M., Nakamura, S., Furu, M., Ito, H., and Matsuda, S. (2015). Posterior tibial slope and femoral sizing affect posterior cruciate ligament tension in posterior cruciate-retaining total knee arthroplasty. Clin Biomech (Bristol, Avon), 30: 676-681. https://doi.org/10.1016/j.clinbiomech.2015.05.006

[17] Zdero, R., Fenton, P., Rudan, J., and Bryant, J. (2001). Fuji film and ultrasound measurement of total knee arthroplasty contact areas. The Journal of arthroplasty, 16: 367-375. https://doi.org/10.1054/arth.2001.21501

[18] Bachus, K. N., DeMarco, A. L., Judd, K. T., Horwitz, D. S., and Brodke, D. S. (2006). Measuring contact area, force, and pressure for bioengineering applications: using Fuji Film and TekScan systems. Med Eng Phys, 28: 483-488. https://doi.org/10.1016/j.medengphy.2005.07.022

[19] American Society for Testing and Materials (2021). Standard Specification for Knee Replacement Prosthesis, ASTM F2083-21. https://www.astm.org/f2083-21.html

[20] Fukuda, I., Pinto, C., Moreira, C., Saviano, A., and Lourenço, F. (2018). Design of Experiments (DoE) applied to Pharmaceutical and Analytical Quality by Design (QbD). Brazilian Journal of Pharmaceutical Sciences, 54: 1-16. https://doi.org/10.1590/s2175-97902018000001006

[21] Dong, Y., Zhang, Z., Dong, W., Hu, G., Wang, B., and Mou, Z. (2020). An optimization method for implantation parameters of individualized TKA tibial prosthesis based on finite element analysis and orthogonal experimental design. BMC Musculoskeletal Disorders, 21: 165. https://doi.org/10.1186/s12891-020-3189-5

[22] Koh, Y.G., Lee, J.A., and Kang, K.T. (2019). Prediction of Wear on Tibial Inserts Made of UHMWPE, PEEK, and CFR-PEEK in Total Knee Arthroplasty Using Finite-Element Analysis. Lubricants, 7: 30. https://doi.org/10.3390/lubricants7040030

[23] Navacchia, A., Rullkoetter, P. J., Schütz, P., List, R. B., Fitzpatrick, C. K., and Shelburne, K. B. (2016). Subject-specific modeling of muscle force and knee contact in total knee arthroplasty. J Orthop Res, 34: 1576-1587. https://doi.org/10.1002/jor.23171

[24] Godest, A. C., Beaugonin, M., Haug, E., Taylor, M., and Gregson, P. J. (2002). Simulation of a knee joint replacement during a gait cycle using explicit finite element analysis. J Biomech, 35: 267-275. https://doi.org/10.1016/s0021-9290(01)00179-8

[25] Abdelgaied, A., Brockett, C. L., Liu, F., Jennings, L. M., Fisher, J., and Jin, Z. (2013). Quantification of the effect of cross-shear and applied nominal contact pressure on the wear of moderately cross-linked polyethylene. Proc Inst Mech Eng H, 227: 18-26. https://doi.org/10.1177/0954411912459423

[26] Anas, M. N. (2014). An Instrumented Insole System for Gait Monitoring and Analysis. International Journal of Online and Biomedical Engineering (iJOE), 10: 30-34. https://doi.org/10.3991/ijoe.v10i6.3971

[27] Galvin, A., Kang, L., Tipper, J., Stone, M., Ingham, E., Jin, Z., and Fisher, J. (2006). Wear of crosslinked polyethylene under different tribological conditions. J Mater Sci Mater Med, 17: 235-243. https://doi.org/10.1007/s10856-006-7309-z

[28] Srinivas, G. R., Deb, A., and Kumar, M. N. (2013). A study on polyethylene stresses in mobile-bearing and fixed-bearing total knee arthroplasty (TKA) using explicit finite element analysis. J Long Term Eff Med Implants, 23: 275-283. https://doi.org/10.1615/jlongtermeffmedimplants.2013008440

[29] Hazir, E., Koc, K., and Hiziroglu, S. (2017). Optimization of sanding parameters using response surface methodology. Maderas: Ciencia y Tecnologia, 19: 407-416. https://doi.org/10.4067/S0718-221X2017005000034

[30] Szivek, J. A., Anderson, P. L., and Benjamin, J. B. (1996). Average and peak contact stress distribution evaluation of total knee arthroplasties. J Arthroplasty, 11: 952-963. https://doi.org/10.1016/s0883-5403(96)80137-9

[31] Takian, W., Rooppakhun, S., Ariyarit, A., and Sucharitpwatskul, S. (2021). Optimal Conformity Design of Tibial Insert Component Based on ISO Standard Wear Test Using Finite Element Analysis and Surrogate Model. Symmetry, 13: 2377. https://www.mdpi.com/2073-8994/13/12/2377

[32] Sathasivam, S., and Walker, P. S. (1999). The conflicting requirements of laxity and conformity in total knee replacement. J Biomech, 32: 239-247. https://doi.org/10.1016/s0021-9290(98)00139-0

[33] Dharia, M. A., Snyder, S., and Bischoff, J. E. (2020). Computational Model Validation of Contact Mechanics in Total Ankle Arthroplasty. J Orthop Res, 38: 1063-1069. https://doi.org/10.1002/jor.24551

[34] Sarwar, A., Srivastava, S., Chu, C., Machin, A., Schemitsch, E. H., Bougherara, H., Bagheri, Z. S. and Zdero, R. (2017). Biomechanical Measurement Error Can Be Caused by Fujifilm Thickness: A Theoretical, Experimental, and Computational Analysis. Biomed Res Int, 2017: 4310314. https://doi.org/10.1155/2017/4310314

8   Authors

Techin Seechaipat is a post-graduate student at the school of biomedical Innovation Engineering, Institute of Engineering, Suranaree University of Technology, Nakhon Ratchasima 30000, Thailand. His research interests included 3D motion analysis, musculoskeletal (MSK) modeling, CAD/ CAE (Reverse Engineering Technology), and biomechanics (email: techin.seechaipat@gmail.com).

Supakit Rooppakhun is an assistant professor and head of CAD/CAE Research Laboratory in School of Mechanical Engineering, Institute of Engineering, Suranaree University of Technology, Nakhon Ratchasima 30000, Thailand. His research interests included Finite Element modeling & simulation, CAD/ CAE (Reverse Engineering Technology), biomechanics, biomedical devices and systems, and vehicle structure design & analysis (email: supakit@sut.ac.th).

Chotchuang Phombut is a Ph.D. candidate in the School of Mechanical Engineering, Institute of Engineering, Suranaree University of Technology, Nakhon Ratchasima 30000, Thailand. His research interests included CAD/ CAE (Reverse Engineering Technology), biomechanics, and biomedical devices and systems (email: chotchuang.p @gmail.com).